



1 **Eurasian autumn snow impact on winter North Atlantic Oscillation**
2 **depends on cryospheric variability**

3
4

5 Martin Wegmann (1), Marco Rohrer (2,3,*), María Santolaria-Otín (4) and Gerrit Lohmann (1)

6 (1) Alfred Wegener Institute, Helmholtz Centre for Polar and Marine Research,
7 Bremerhaven, Germany

8 (2) Oeschger Centre for Climate Change Research, University of Bern, Bern, Switzerland

9 (3) Institute of Geography, University of Bern, Bern, Switzerland

10 (4) Institut des Géosciences de l'Environnement, Université Grenoble-Alpes, France

11 (*) now at: Axis Capital, Zurich, Switzerland

12

13 **Abstract:**

14 In recent years, many components of the connection between Eurasian autumn snow cover
15 and wintertime North Atlantic Oscillation (NAO) were investigated, suggesting that
16 November snow cover distribution has strong prediction power for the upcoming Northern
17 Hemisphere winter climate. However, non-stationarity of this relationship could impact its
18 use for prediction routines. Here we use snow products from long-term reanalyses to
19 investigate interannual and interdecadal links between autumnal snow cover and
20 atmospheric conditions in winter. We find evidence for a negative NAO tendency after
21 November with a strong west-to-east snow cover gradient, which is valid throughout the
22 last 150 years. This correlation is linked with a consistent impact of November snow on a
23 slowed stratospheric polar vortex. Nevertheless, interdecadal variability for this relationship
24 shows episodes of decreased correlation power, which co-occur with episodes of low
25 variability in the November snow index. We find that the same is also true for sea ice as an
26 NAO predictor. The snow dipole itself is associated with reduced Barents-Kara sea ice
27 concentration, increased Ural blocking frequency and negative temperature anomalies in
28 eastern Eurasia. Increased sea ice variability in recent years is linked to increased snow
29 variability, thus increasing its power in predicting the winter NAO.

30

31 **Keywords: SNOW, NAO, SEA ICE, VARIABILITY, PREDICTION**

32



33 **1. Introduction**

34 As the leading climate mode to explain wintertime climate variability over Europe (**Thompson**
35 **and Wallace 1998**), the North Atlantic Oscillation (NAO) has been extensively studied over
36 the last decades (**Wanner et al. 2001, Hurrell and Deser 2010, Moore and Renfrew 2012,**
37 **Pedersen et al. 2016, Deser et al. 2017**). The NAO has been defined as the strength of the
38 pressure gradient between Iceland (representing the edge of the polar front) and the Azores
39 (representing the subtropical high ridge). The sign of the NAO is related to weather and climate
40 patterns stretching from local to continental scales. Since its configuration has severe
41 socioeconomic, ecological and hydrological impacts for adjacent continents, seasonal to
42 decadal predictions of the state of the winter NAO are high priority research for many climate
43 science centers (**Jung et al. 2011, Kang et al. 2014, Scaife et al. 2014, Scaife et al. 2016,**
44 **Smith et al. 2016, Dunstone et al. 2016, Wang et al. 2017, Athanasiadis et al. 2017**).

45 Together with the rapid warming of the Arctic and the increased frequency of severe winters
46 over Eurasia and North America (**Yao et al. 2017, Cohen et al. 2018, Kretschmer et al. 2018,**
47 **Overland and Wang 2018**), recent studies highlighted the state of the Northern Hemispheric
48 cryosphere as a useful predictor for the boreal wintertime (DJF) NAO (**Cohen et al. 2007,**
49 **Cohen et al. 2014, Vihma 2014, Garcia-Serrano et al. 2015, Cohen 2016, Orsolini et al.**
50 **2016, Crasemann et al. 2017, Warner 2018**). Although both systems seem to be connected
51 (**Cohen et al. 2014, Furtado et al. 2016, Gastineau et al. 2017**), the emerging main hypothesis
52 connects reduced autumn Barents-Kara sea ice concentration and increased Siberian snow
53 cover with a negative NAO state in the following winter months (**Cohen et al. 2014**).

54 The proposed mechanism behind this hypothesis is a multi-step process, starting with autumn
55 sea ice loss for the European Arctic, followed by altered tropospheric circulation due to elevated
56 Rossby wave numbers, vertical propagation of said Rossby waves upward into the stratosphere
57 and consequently a weakening of the polar vortex (see **Cohen et al. 2014** for an in depth
58 discussion). With the weakening (or the reversal) of the polar vortex, a stratospheric warming
59 signal manifests. This signal propagates slowly back into the troposphere, where it is expressed
60 as a negative NAO, connected to the concurrent cold winters for Eurasia (**Kretschmer et al.**
61 **2018**).

62 In recent years, many components of this pathway were investigated, especially concerning the
63 increased frequency of cold winters over Europe and the emergence of the counter-intuitive
64 “Warm Arctic – cold continent” (WACC) pattern over Eurasia (**Petoukhov and Semenov**



65 **2010, Vihma 2014)**. However, there remains substantial uncertainty about the impact of Arctic
66 sea ice in terms of location (**Zhang et al 2016, Luo et al 2017, Screen 2017, Kelleher and**
67 **Screen 2018)**, timing (**Honda et al 2009, Overland et al 2011, Inoue et al 2012, Suo et al**
68 **2016, , Sorokina et al 2016, King et al 2016, Screen 2017, Wegmann et al 2018a, Blackport**
69 **and Screen 2019)** or if sea ice can be used as a predictor/forcing at all based on the contrasting
70 result of model studies (**McCusker et al. 2016, Collopy et al. 2016, Pedersen et al. 2016,**
71 **Boland et al. 2017, Crasemann et al. 2017, Ruggieri et al. 2017, Garcia-Serrano et al. 2017,**
72 **Francis 2017, Screen et al. 2018, Mori et al. 2019, Hoshi et al. 2019, Blackport et al. 2019,**
73 **Romanowksy et al. 2019)**.

74 The interplay between Arctic sea ice and Siberian snow is much less explored. **Ghatak et al.**
75 **(2010)** showed that reduced autumn polar sea ice leads to the emergence of increased Siberian
76 winter snow cover, especially so in the eastern part of Eurasia. This dipole signal was amplified
77 in coupled climate model runs for the 21st century, where sea ice is substantially diminished. In
78 an observational study, **Yeo et al. (2016)** point out that the moisture influx from the open Arctic
79 ocean into the Eurasian continent contributes to the increase of snow cover, a mechanism that
80 **Wegmann et al. (2015)** describe. **Gastineau et al. (2017)** found that reduced sea ice is
81 connected to a distinct November snow dipole over Eurasia, both in reanalysis and model data.
82 They further state, that the snow component is a statistically more powerful predictor for the
83 atmosphere in the following winter. This relationship was also found in a range of climate
84 models, albeit with weaker links. **Xu et al. (2019)** found the same correlation in observational
85 and model data, however looking at winter climate only. Based on their analysis, the authors
86 state that the enhanced snow cover in winter is a product of the negative NAO rather than a
87 precursor. **Sun et al. (2019)** highlight the importance of elevated North Atlantic sea surface
88 temperatures for the development of a Eurasian snow dipole in autumn. This warming of the
89 North Atlantic favors increased Rossby wave numbers, eventually forming a high pressure
90 anomaly over the Ural Mountains, transporting cold air masses towards the south of its eastern
91 flank.

92 The possible impact of the Siberian snow on the stratosphere and eventually on the NAO is
93 well summarized in **Henderson et al. (2018)**. Although observational NAO prediction studies
94 with Siberian snow showed great success in the past (**Cohen and Entekhabi 1999, Saito et al.**
95 **2001, Cohen et al. 2007, Cohen et al. 2014, Han and Sun 2018)**, links between snow and the
96 stratosphere still seems to be missing or too weak in model studies (**Furtado et al. 2015,**
97 **Handorf et al. 2015, Tyrrell et al. 2018, Gastineau et al. 2017, Peings et al. 2017)**, whereas



98 nudging realistic snow changes to high resolution models seems to improve the prediction
99 power (Orsolini and Kvamsto 2009, Orsolini et al. 2016, Tyrrell et al. 2019). Moreover,
100 even though the stratosphere–surface connection is now reasonably well established
101 (Kretschmer et al. 2018), the timing and location of the snow cover used for the prediction is,
102 as with sea ice, still debated (Yeo et al. 2016, Gastineau et al. 2017). As an additional caveat,
103 Peings et al. (2013) and more recently Douville et al. (2017), showed that the proposed autumn
104 snow-to-winter NAO relationship is non-stationary for the 20th century. A possible modulator
105 for that relationship might be the phase of the Quasi Biennial Oscillation (QBO) (Tyrrell et al.
106 2018, Peings et al. 2017, Douville et al. 2017). Peings (2019) argues that neither snow nor sea
107 ice anomalies trigger the stratospheric conditions needed to produce winter extremes and that
108 instead high tropospheric blocking frequency over Northern Europe leads to the cryosphere
109 anomalies.

110 Here, we follow up on the consequences of recent studies (Han and Sun 2018, Gastineau et
111 al. 2017) who point out the predictor strength of the November snow cover dipole for the
112 following winter month, to revisit the question of a) non-stationarity in the 20th century, b)
113 importance of snow versus sea ice as predictor and c) possible precursors/modulators of the sea
114 ice–snow–stratosphere link. With this we aim to contribute to the understanding of impacts of
115 cryosphere variability on midlatitude circulation (Francis 2017, Henderson et al. 2018,
116 Blackport et al. 2019). To this end, we utilize centennial reanalyses and reconstruction data,
117 where we focus on the transition from October to November to DJF to facilitate the idea of
118 seasonal prediction.

119 This paper is organized as follows: Section 2 describes the data and methods used. In section
120 3, we introduce the snow cover indices and their interannual prediction value. Section 4
121 investigates interdecadal shifts in the correlation between snow cover and NAO as well as
122 possible determining factors. The results are discussed in section 5 and finally summarized in
123 section 6.

124 2. Data and Methods

125 a. Atmospheric reanalyses

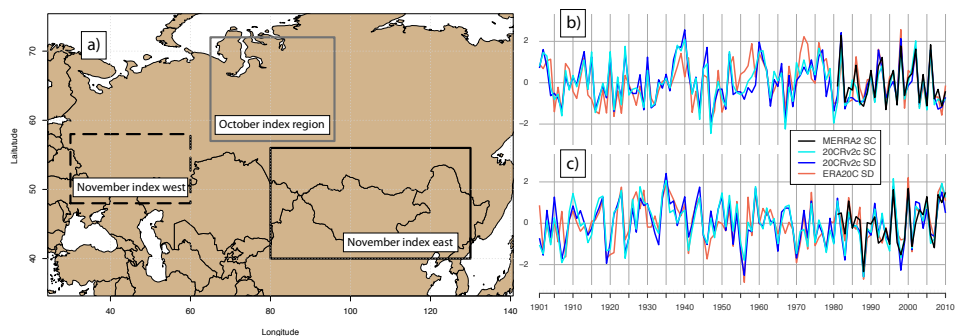
126 To evaluate long-term reanalyses, we use snow cover, snow depth and atmospheric properties
127 from the MERRA2 reanalysis (Gelaro et al. 2017). MERRA2 has a dedicated land surface
128 module and was found to reproduce local in-situ snow conditions over Russia very well



129 (Wegmann et al. 2018b). For an in-detail description of how MERRA2 computes snow
130 properties see e.g. Orsolini et al. (2019).

131 To cover the 20th century and beyond, we include two long-term reanalyses in this study,
132 namely the NOAA-CIRES 20th century reanalysis Version 2c (20CRv2c) (Cram et al. 2015)
133 as well as the Centre for Medium-Range Weather Forecasts (ECMWF) product ERA-20C (Poli
134 et al. 2016). From the ERA-20C product we use snow depth, whereas from 20CRv2c we
135 investigate snow depth and snow cover. Both reanalyses were found to represent interannual
136 snow variations over Eurasia remarkably well. For an in-depth discussion of their performance
137 and their technical details concerning snow computation see Wegmann et al. (2017). We also
138 performed the same analysis using the coupled ECMWF reanalysis CERA-20C (Laloyaux et
139 al., 2018), but found no added knowledge gain over ERA-20C. Thus, we do not include CERA-
140 20C in any further analysis.

141 We use these three reanalysis products to extend the October and November index proposed by
142 Han and Sun (2018) into the past, where the November index is in essence the snow dipole
143 found by Gastineau et al. (2017) using maximum covariance analysis (Figure 1). Where the
144 October index is just calculated as field average snow cover, the November index is computed
145 as difference between the eastern and the western field average. It should be noted, that Han
146 and Sun (2018) found the November index to be linked to a negative NAO and colder Eurasian
147 near-surface temperatures, whereas the October index was correlated with warmer-than-usual
148 temperatures over Eurasia and a southward-shifted positive DJF NAO. However, since many
149 studies focus on Northern Eurasian October snow cover as the predictor for winter climate, we
150 will include it nonetheless. MERRA2 and 20CRv2c offer snow cover as well as snow depth as
151 a post-process output, however ERA-20C only offers snow depth. We refrain from converting
152 it to snow cover ourselves, but found the index based on snow depth to be extremely similar
153 (also see Supplementary Figure 1) to the same index using snow cover. All snow indices are
154 normalized and linearly detrended with respect to their overall time period. Generally, we found
155 the long term reanalyses to be of comparable quality of MERRA2 during the overlapping
156 periods.



157

158 Figure 1: a) Regions for October and November snow index used in this study. b) Linearly
159 detrended and normalized October snow index comparison for the 20th century for snow cover
160 (SC) and snow depth (SD) variables. c) same as b) but for the November snow dipole.

161 Besides snow properties we use atmospheric and near-surface fields from all three reanalyses.
162 Moreover, as **Douville et al. (2017)**, we use the field averaged (60°–90° N) 10 hectopascal
163 (hPa) geopotential height (GPH) anomalies in ERA-20C as a surrogate for polar vortex (PV)
164 strength. Although ERA-20C only assimilates surface pressure, correlation between this
165 stratospheric index in ERA-20C and MERRA2 during the overlapping time periods is above
166 0.9.

167 The ERA20C 10 hPa November–December mean GPH shows remarkable interannual
168 agreement with state-of-the-art reanalyses that assimilate upper air data for the period 1958–
169 2010 (see Supplementary Figure 2). Moreover, MERRA2 and ERA20C 10 hPa GPH anomalies
170 agree best over the northern polar regions with correlation coefficients of >0.9 for the period
171 1981–2010 (see Supplementary Figure 2). This fact supports the extended value of the ERA20C
172 polar stratosphere. Before 1958, the quality of the ERA20C stratosphere is difficult to assess,
173 but the comparison with reconstructions of 100 hPa GPH zonal means shows very good
174 agreement for late autumn and winter months (see Supplementary Figure 3). As the 20CRv2c
175 ensemble mean dilutes the interannual variability signal back in time with increased variability
176 within the ensemble members, we use the deterministic run of ERA20C for the following
177 stratosphere analyses.

178 We use 6-hourly 500 hPa GPH fields (GPH500) to calculate monthly blocking frequencies
179 according to **Rohrer et al. (2018)**. Blockings are computed according to the approach
180 introduced by **Tibaldi and Molteni (1990)** and are defined as reversals of the meridional
181 GPH500 gradient. In accordance to **Scherrer et al. (2006)** the one-dimensional **Tibaldi and**



182 **Molteni (1990)** algorithm is extended to the second dimension by varying the latitude between
183 35° and 75° instead of a fixed latitude:

184 i) GPH500 gradient towards pole: $GPH500G_P = \frac{GPH500_{\varphi+d\varphi} - GPH500_{\varphi}}{d\varphi} < -10 \frac{m}{^{\circ}lat}$ (1)

185

186 ii) GPH500 gradient towards equator: $GPH500G_E = \frac{GPH500_{\varphi} - GPH500_{\varphi-d\varphi}}{d\varphi} > 0 \frac{m}{^{\circ}lat}$ (2)

187

188 Blocks by definition are persistent and quasi-stationary high-pressure systems that divert the
189 usually prevailing westerly winds in the mid-latitudes. They influence regional temperature and
190 precipitation patterns for an extended period. Therefore, not all blocks that fulfill above
191 mentioned two conditions are retained. We only include blocks that have a minimum required
192 lifetime of 5 days and a minimum overlap of the blocked area of 70% ($A_{t+1} \cap A_t > 0.7 * A_t$)
193 in our blocking catalog. This largely follows the criteria defined by **Schwierz et al. (2004)**.

194 b) Climate reconstructions

195 To be as independent as possible with regards to the reanalyses we use a wide array of climate
196 index reconstructions for the 20th century:

- 197 • Atlantic Multidecadal Oscillation (AMO): For the AMO index we take October values
198 based on the **Enfield et al. (2003)** study. We choose October to allow for a certain
199 feedback lag with the atmosphere and to have decent prediction value for the upcoming
200 snow and NAO indices.
- 201 • El Niño – Southern Oscillation (ENSO): We chose the ENSO3.4 reconstruction based
202 on the HadISSTv1 **Rayner et al. (2003)** SSTs. As with the AMO, we select October
203 values to allow for a reaction time in the teleconnections.
- 204 • North Atlantic Oscillation (NAO): We use the extended **Jones et al. (1997)** NAO index
205 for DJF from the Climate Research Unit (CRU).
- 206 • Sea Ice: We use the monthly sea ice reconstruction by **Walsh et al. (2017)** which covers
207 the period 1850–2013 to create a Barents-Kara (65–85°N, 30–90°E) sea ice index for
208 November.

209 3. Results

210 a. Interannual links

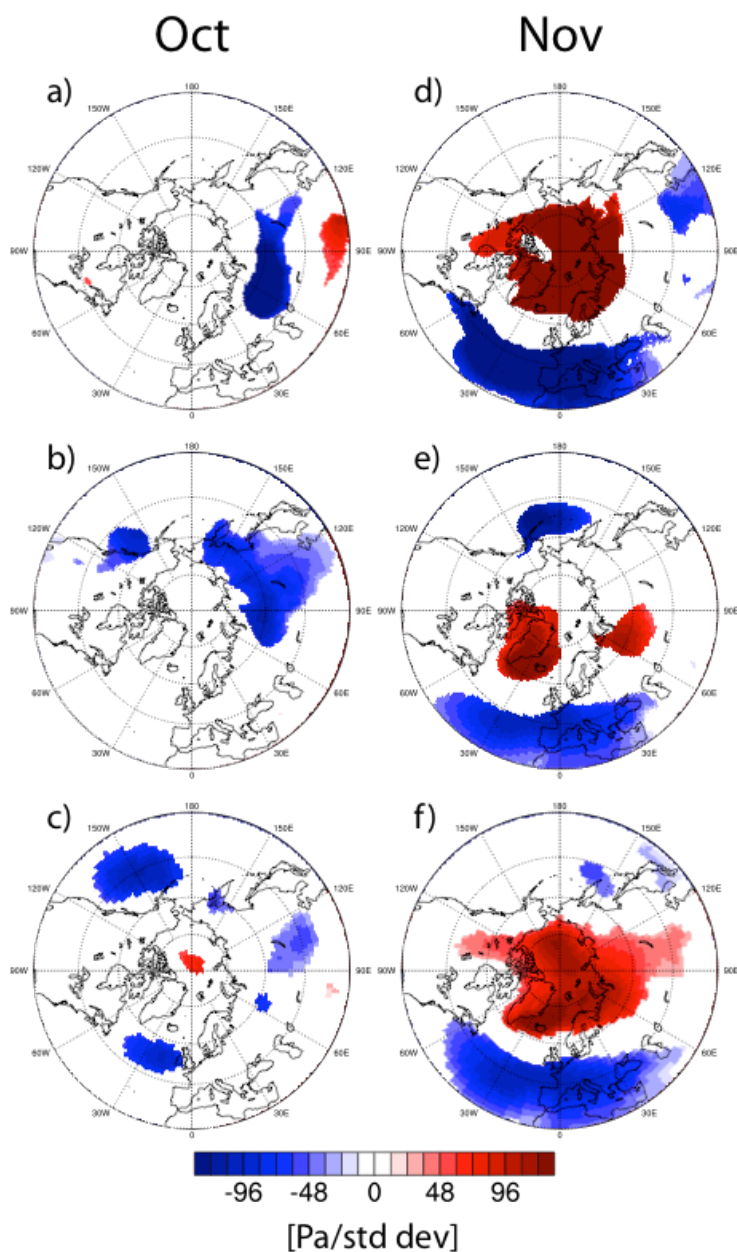


211 In the following paragraphs we investigate the year-to-year relationship between the snow
212 indices and the following winter SLP fields. For this we use MERRA2 for a 35-year-long
213 window ranging from 1981–2015, ERA20C for a 110-year-long window ranging from 1901–
214 2010 and 20CRv2c for a 160-year-long window ranging from 1851–2010.

215 Figure 2 shows the linear regression fields of DJF SLP anomalies projected onto the respective
216 snow indices in October and November. For October, we find no NAO-like pressure anomaly
217 appears to be significantly correlated with the snow index in any of the three reanalysis products
218 and respective time windows (Figure 2a,b,c). Instead, negative SLP anomalies dominate
219 Northern Eurasia in MERRA2, with high pressure anomalies towards the Himalayan Plateau.
220 The 110-year-long regression in ERA20C shows significant negative anomalies over the Asian
221 part of Russia, reaching as far south as Beijing. A second significant negative SLP pattern
222 appears along the Pacific coast of Canada. Finally, SLP anomalies in 20CRv2c support the main
223 SLP patterns shown by ERA20C, but reduce the extent of negative anomalies over Eurasia and
224 increase the extent of the negative anomalies over the North Pacific.

225 The DJF SLP anomaly patterns change substantially when projected onto the November snow
226 index (Figure 2d,e,f). All three reanalysis products show negative NAO-like pressure anomalies
227 with significantly positive anomalies over Iceland and the northern North Atlantic and
228 significantly negative anomalies south of ca. 45° N, including Portugal and the Azores. As
229 expected, MERRA2 shows the strongest anomalies due to the shorter regression period,
230 however interestingly ERA20C, with the 110-year long analysis period, shows less large-scale
231 significance for positive anomalies in high latitudes compared to the 150-year-long
232 investigation period in 20CRv2c (even though non-significant anomalies cover roughly the
233 same area as in 20CRv2c (not shown)). This can hint towards decadal variations in the strength
234 of the regression, but could also be due to biases in the reanalyses.

235 To check for such biases we compared all reanalyses with the SLP reconstruction dataset
236 HadSLP2r (Allen and Ansell 2006), and found that for the regression analysis using the time
237 period 1901–2010, 20CRv2c overestimates the polar sea level pressure response, whereas
238 ERA20C is much closer to HadSLP2r (See Supplement Figure 4). This would indeed support
239 the notion of decadal variations in the strength of the relationship between predictor and
240 predictand. However, it is worth highlighting that this overestimation for 20CRv2c is not visible
241 for the 1851–2010 period, where the regression anomalies resemble HadSLP2r much closer.



242

243 *Figure 2: DJF sea level pressure [Pa/std dev] anomalies projected onto snow indices in October (left) and November (right)*
244 *for a) MERRA2 covering 1981–2015, b) ERA20C covering 1901–2010 and c) 20CRv2c covering 1851–2010.*
245 *Only anomalies >95% significance level are shown.*

246

247 We investigate other possible predictors for wintertime NAO via regressed anomalies onto the
248 November Barents-Kara-Sea (BKS) ice concentration, November–December mean polar GPH



249 at 10 hPa, October AMO and October ENSO indices (Figure 3). The periods for MERRA2 and
250 ERA20C are identical as for Figure 2, whereas the anomaly plots for 20CRv2c are using the
251 maximum period covered in the reconstructions, namely 1851–2010 in the sea ice
252 reconstruction, 1856–2010 in the AMO reconstruction, 1901–2010 for the polar 10 hPa GPH
253 index taken from ERA20C, and 1870–2010 for the ENSO reconstruction.

254 As can be seen from Figure 3, the 35-year-long analysis in MERRA2 shows November sea ice
255 concentration and early winter stratospheric heights to regress a similar SLP pattern than the
256 November snow index. Positive SLP anomalies over Iceland and Greenland combined with
257 negative anomalies over Southern Europe and the adjacent North Atlantic shape a negative
258 NAO-like pattern in DJF (Figure 3a). On the other hand, the interannual signals in the October
259 AMO and ENSO indices do not point towards such a pressure distribution. The small
260 interannual changes and low frequency of the AMO combined with the short sample period
261 prohibit most of the significance, only Southern Eurasia shows regions with elevated SLP.
262 Anomalies regressed on the ENSO index show, as expected, significance mostly for the North
263 Pacific and North American region.

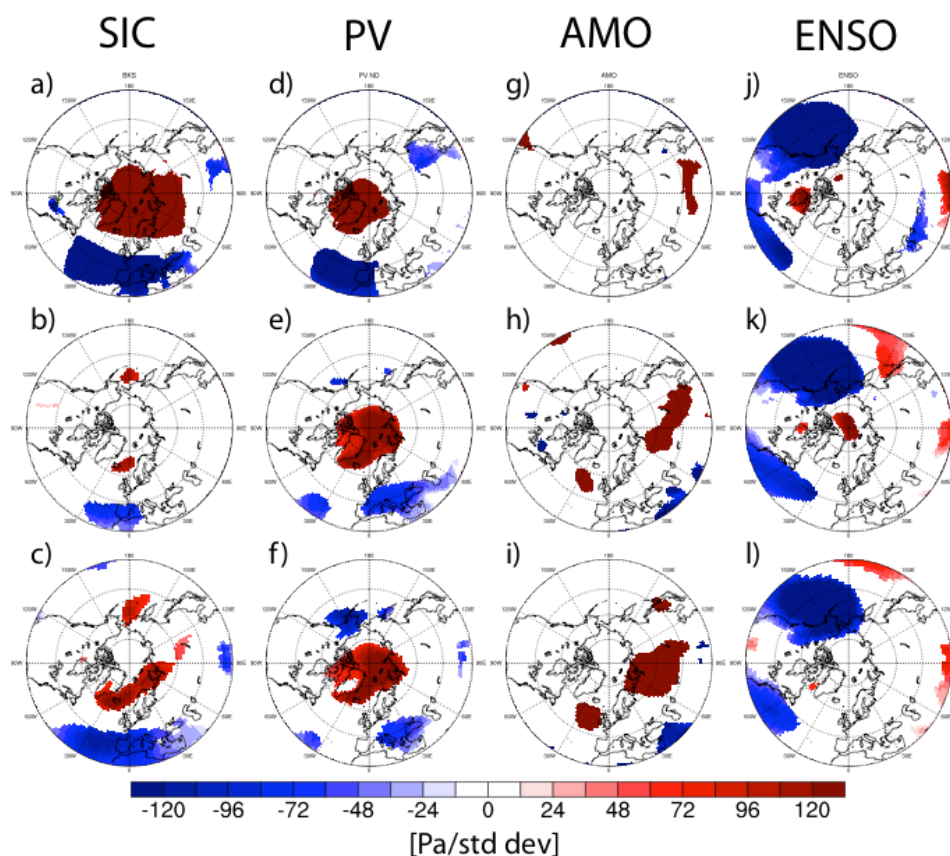
264 Looking at the regression patterns in the centennial reanalyses, the NAO-like pattern in the SLP
265 anomalies regressed onto sea ice and stratospheric GPH can still be seen, however the extent
266 and strength is substantially reduced compared to MERRA2 as well as compared to the
267 regression using November snow as predictor. Again, ERA20C shows a decrease in the
268 significant anomalies regressed onto sea ice compared to 20CRv2c, with possible reasons
269 already discussed above. Elevated geopotential heights at 10 hPa consistently increases polar
270 sea level pressure in the following winter months, however the impact over the European and
271 North Atlantic domain is weak.

272 SLP anomalies regressed onto the AMO index show significant positive SLP regions for large
273 parts of Eurasia as well as positive anomalies over the North Atlantic west of Great Britain.
274 Interesting to note in 20CRv2c is the very strong high-pressure anomaly reaching from the BKS
275 to the southern part of the Ural mountains, a prominent feature often found for years with
276 positive AMO and negative sea ice concentration, frequently linked to a high frequency of Ural
277 blockings (UBs). SLP distribution after El Niño events does not change considerably
278 irrespective of the dataset and time period used. A strong Pacific signal shows the northern part
279 of the Pacific-North American pattern (PNA) with negative SLP anomalies over the eastern
280 North Pacific.

281



282



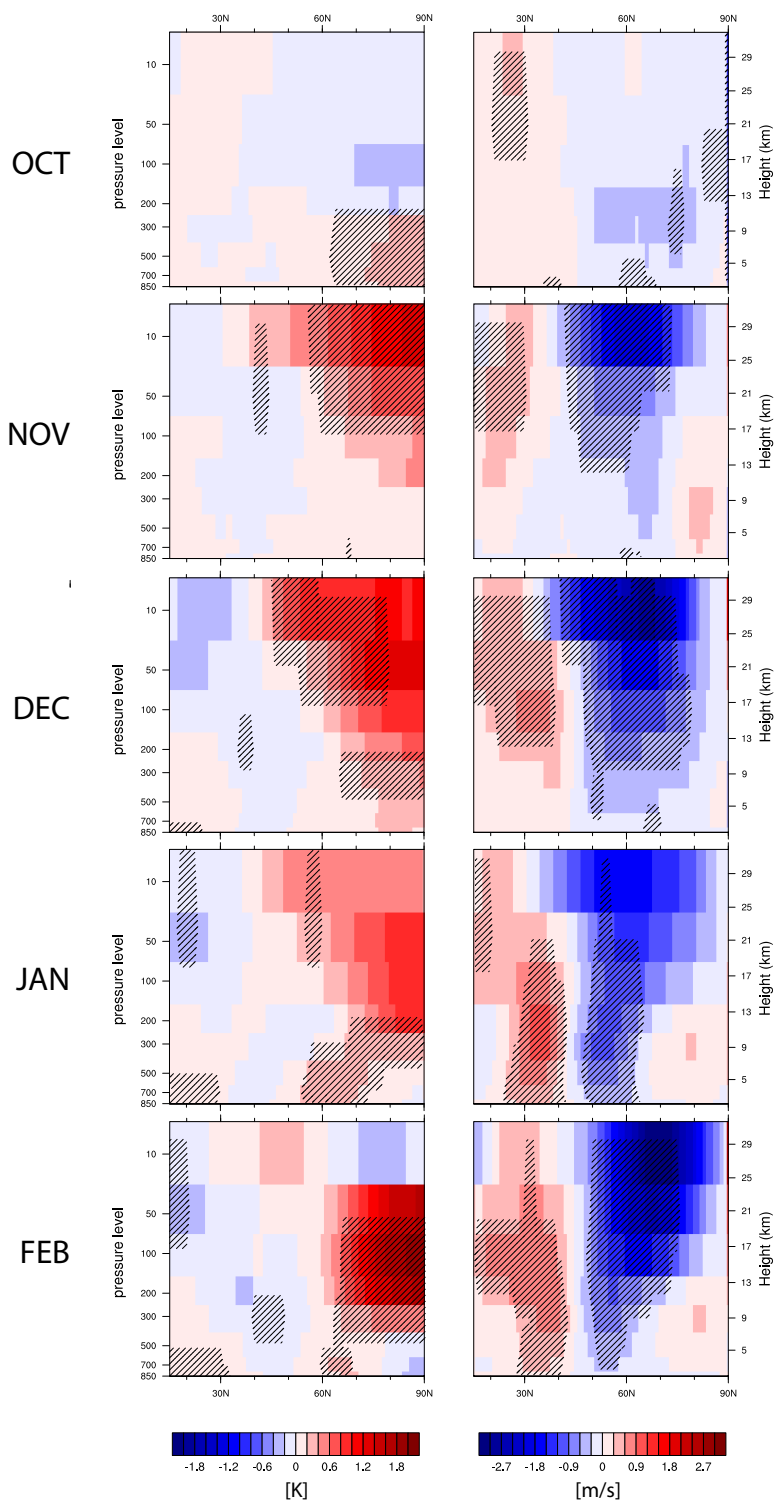
283

284 *Figure 3: DJF sea level pressure [Pa/std dev] anomalies projected onto BKS ice concentration in November (far left), polar*
285 *10 hPa GPH November December mean (left), October AMO (right) and October ENSO indices (far right) for adjg) MERRA2*
286 *covering 1981–2015, behk) ERA20C covering 1901–2010 and cfil) 20CRv2c covering 1851–2010. Regression values for BKS*
287 *ice concentrations were multiplied by minus one to increase comparability. Only anomalies >95% significance level are shown.*

288 To investigate the vertical development of climate anomalies connected with the November
289 snow dipole, Figure 4 shows the zonal mean anomalies of zonal wind and temperature in
290 ERA20C projected onto the ERA20C November snow index (for an evaluation with an upper-
291 air reconstruction see supplementary Figure 5). The temporal evolution of the anomalies
292 ranging from October to February shows that stratospheric warming occurs simultaneously
293 within the same month as a positive snow cover dipole, with no stratospheric warming leading
294 that development. Instead, significant surface warming is shown between 60°–90°N for
295 October. The warming signal then dominates the stratosphere and upper troposphere in
296 December, after which the strongest anomalies subside into the lower stratosphere and
297 tropopause in January and February. This development of atmospheric temperatures is mirrored



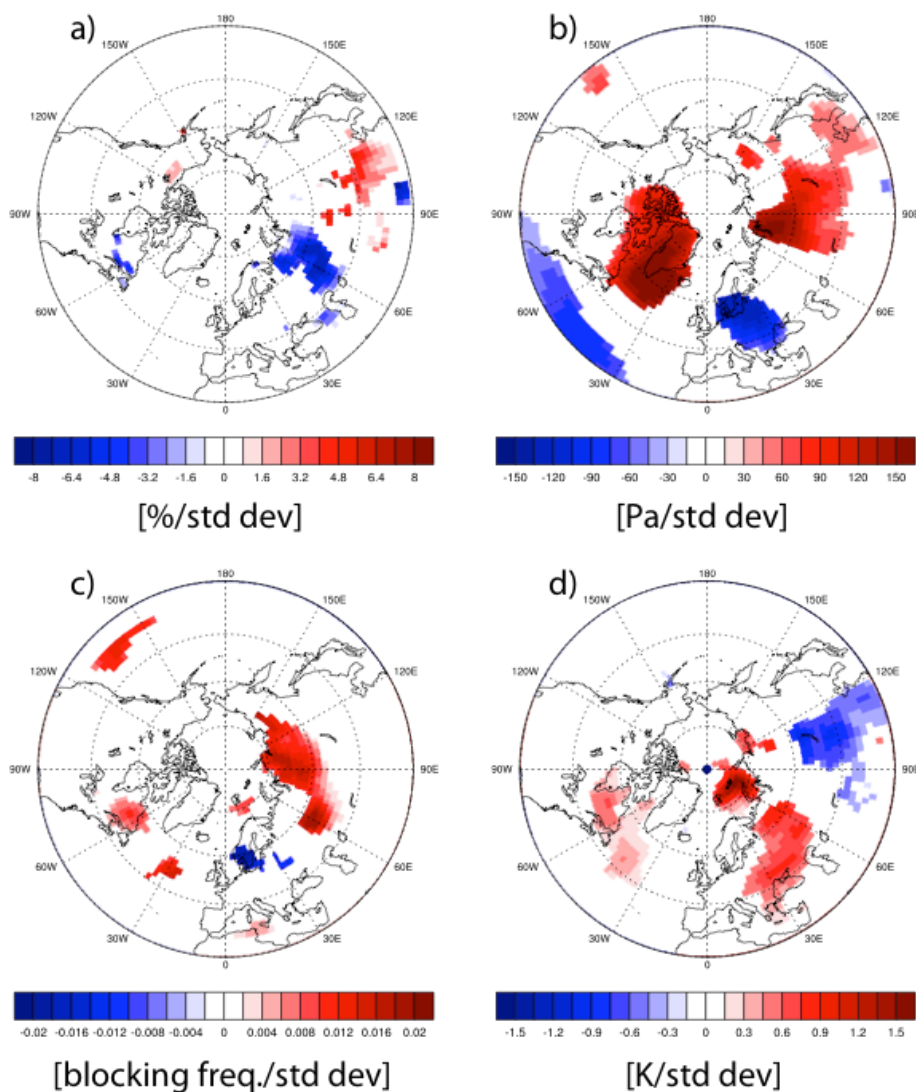
298 in the evolution of the polar vortex, where a reduction of the polar vortex and strengthening of
299 the subtropical jet is seen together with the emergence of the November snow dipole, after
300 which the region of strongest anomalies migrates from the upper stratosphere to the upper
301 troposphere.





303 *Figure 4: Zonal mean (180°E–180°W, 15°N–90°N) left) temperature anomalies and right) zonal mean zonal wind anomalies*
304 *projected onto snow indices in November for ERA20C covering 1901–2010. Shading indicates 95% significance level.*

305 To address the physical reasons as to how the low sea ice and high snow indices are connected,
306 climate anomalies regressed onto BKS ice concentrations for November (Figure 5). Compared
307 to factors such as AMO and ENSO, BKS sea ice shows a distinct snow cover dipole coinciding
308 with a high-pressure anomaly over the BKS and the northern Ural mountains, which supports
309 a regional atmospheric blocking and a cold air advection on its eastern flank. This cold air
310 anomaly is able to support the snow cover over eastern Eurasia, while relatively warm
311 temperatures reduce the snow cover over eastern Europe. It should be noted that October BKS
312 ice concentration shows qualitatively the same pattern for November snow cover anomalies
313 (not shown), however not statistically significant.



314

315 *Figure 5: 20CRv2c November anomalies projected onto BKS ice concentration in November covering 1851–2010. a)*
316 *November snow cover [%/std dev] anomalies projected onto BKS ice concentration in November, b) November SLP [Pa/std*
317 *dev] anomalies projected onto BKS ice concentration in November, c) November atmospheric blocking [blocking per time*
318 *unit/std dev] anomalies projected onto BKS ice concentration in November and d) November 2m temperature [K/std dev]*
319 *anomalies projected onto BKS ice concentration in November. Only anomalies >95% significance level are shown.*

320

b. Interdecadal links

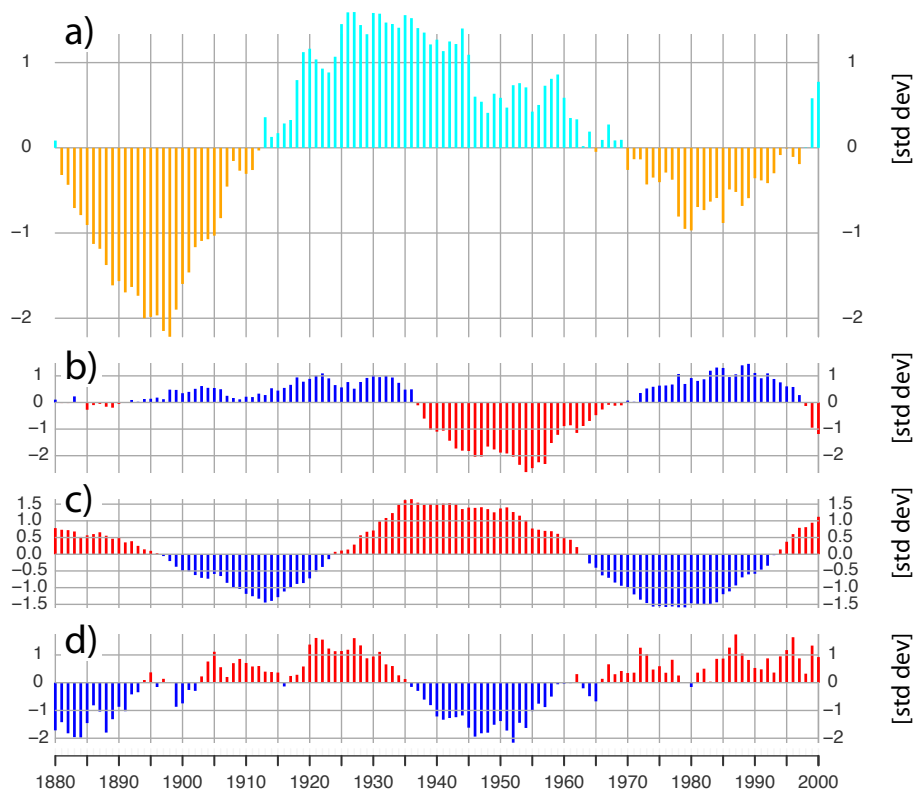
321

The interdecadal evolution of the November snow index is shown in Figure 6. 21-year running
322 means of the normalized time series of ENSO, AMO, BKS ice and snow hint towards a
323 multidecadal frequency, similar in wave length to the AMO and BKS ice anomalies. Even
324 though we refrain from correlating these time series due to the the 21-year filter (**Trenary and**



325 **DelSole, 2016**), we find the possible mechanism behind it, which was outlined in the previous
326 section, to be physically plausible. As **Luo et al. (2016)** point out, warm North Atlantic water
327 reduces the BKS ice concentration which in turn favors the formation of high pressure over the
328 Ural mountains and with that, cold air advection towards eastern Eurasia. It should be noted
329 however, that the AMO and the November snow index are slightly out-of-phase between 1880
330 and 1920. Possible reasons for that will be examined in the discussion section, but we want to
331 highlight the strong La Niña events at the end of the 19th century as well as the strong El Niño
332 events between 1920–1940 that seem to have enough power to influence European climate
333 (**Brönnimann et al. 2004, Brönnimann et al. 2007, Domeisen et al. 2018**).

334



335

336 *Figure 6: 21-year running means of a) November snow index from 20CRv2c, b) November BKS ice concentration, c) October*
337 *AMO and d) October ENSO reconstruction.*



338 The more critical question is the interdecadal evolution of the relationship between the predictor
339 and the predictand. Similar to **Peings et al. (2013)** and **Douville et al. (2017)**, we apply a 21-
340 year running correlation covering the period 1901–2010 to examine the stationarity of the
341 relationship and differences between 20CRv2c and ERA20C.

342 Figure 7 summarizes the correlation over time for multiple pairs of climate variables. As Figure
343 7b points out, the sign of the November snow to winter NAO relationship in 20CRv2c is
344 negative throughout the whole 20th century. Periods with negative correlations can be found at
345 the beginning and the end of the century, with relatively weak correlation during the 1930s and
346 1970s. In ERA20C, these periods are actually marked by positive correlations, indicating a non-
347 stationary relationship between these two variables. Even stronger decadal variability can be
348 seen for the running correlations between the October snow index and winter NAO tendency
349 (Figure 7a), with periods of pronounced negative correlations during the early 20th century
350 Arctic warming and the 1980s. A recently emerging relationship can be seen in Figure 7c
351 between BKS ice reduction and the formation of a negative NAO signal in the following winter.
352 Even though the beginning of the 20th century showed the same sign for this correlation,
353 decades of positive correlation follow up and last until the late 1970s.

354 Together with the emergence of the sea ice to NAO relationship, the negative correlations
355 between BKS sea ice and November snow index as well as between stratospheric warming and
356 winter NAO strengthen towards the end of the 20th century. This strengthening is also found in
357 ERA20C for the correlation between November snow and a following stratospheric warming,
358 where 20CRv2c shows consistently positive correlation values throughout the 20th century.

359 Overall, the 20CRv2c November snow index shows a more stationary relationship with
360 tropospheric and stratospheric winter circulation than ERA20C. Possible explanations for this
361 behavior will be discussed in the following section.



362

363 *Figure 7: 21-year centered running correlation time series between a) October snow index and DJF NAO, b) November snow index and DJF NAO, c) November snow index and mean November-December polar 10 hPa GPH index, d) November snow index and November BKS ice concentration, e) November BKS ice concentration*-1 and DJF NAO and f) mean November-December polar 10 hPa GPH and DJF NAO index. Black dashed line indicating the 95% confidence level for a two-sided*
364
365
366
367 *students T-test assuming independence and normal distribution.*

368

4. Discussion



369 We used a variety of reanalyses and reconstructions to address some of the open questions
370 regarding the relationship between Eurasian snow cover and the state of the NAO in the
371 following winter. We followed up on the findings of **Gastineau et al. (2017)** as well as **Han**
372 **and Sun (2018)** who pointed out the distinct November Eurasian snow cover dipole pattern
373 and its prediction skill for the winter NAO during recent decades in reanalyses. Given the
374 importance for seasonal prediction, we address the question of stationarity of said relationship
375 as well as its context within other popular Northern Hemispheric predictors by utilizing
376 centennial snow cover, SST and sea ice concentration indices.

377 Investigating interannual relationships, we could show that the October snow index shows no
378 skill in predicting the NAO state whereas the November snow index, representing the west-to-
379 east gradient of snow cover, shows a strong negative statistical relationship for the following
380 winter NAO. Our findings also support results shown by **Gastineau et al. (2017)**, indicating
381 that reduced BKS sea ice shows a similar response in DJF SLP anomalies, however its statistical
382 importance, and therefore quality as being the prime predictor, is less than the November snow
383 index (see Supplementary Table 1 for partial correlations). SST indices with low interannual
384 variability, such as AMO and ENSO indices, did not correlate with the DJF NAO state.

385 The question remained, how stationary this relationship between Eurasian snow and the
386 wintertime NAO is over time. **Peings et al. (2013)** and the follow up study by **Douville et al.**
387 **(2017)** found that the October and October–November mean snow cover over a broader region
388 of Northern Eurasia, and its relationship to the wintertime NAO is indeed not stationary over
389 time. We could show that by using the November snow dipole, we could extend the results of
390 **Han and Sun (2018)** and display a very significant (95% significance and higher) negative
391 interannual correlation with wintertime NAO, going beyond the satellite era up until the mid-
392 19th century. Moreover, we highlight the strong correlation between November snow and
393 stratospheric warming, supporting the general idea of the physical mechanism proposed by
394 **Cohen et al. (2014)** and supporting the recent findings of **Gastineau et al. (2017)** and **Douville**
395 **et al. (2017)**.

396 In accordance to **Sun et al. (2019)**, decadal variability of the November snow cover index seems
397 mostly dominated by low frequency variability in the AMO and subsequently reduced or
398 increased polar sea ice concentration. This mechanism is also supported by the results of **Luo**
399 **et al. (2016)**, who highlighted the decadal relationship between a positive AMO, reduced sea
400 ice and increased Ural blocking. Looking at this mechanism on an interannual basis, we show



401 a robust strengthening of the November snow dipole with decreasing BKS ice concentration,
402 circulation changes over the BKS region and consequently cold air advection towards the
403 eastern part of the snow dipole region. With this, our results support recent studies, which point
404 out the counterintuitive mechanism of Arctic warming and increased continental snow cover
405 via sea ice reduction and circulation changes (Cohen et al. 2014, Wegmann et al. 2015, Yeo
406 et al. 2016, Gastineau et al. 2017).

407 Peings (2019) performed model experiments with nudged November Ural blocking fields, BKS
408 ice and snow anomalies. The author found that UB events are not triggered by reduced sea ice,
409 but in fact lead sea ice decrease. Moreover, more November snow alone did not lead to an
410 increase in blocking frequency, nor to a stratospheric warming. The study highlights the UB
411 events as primary predictor for a negative NAO and the Warm Arctic-cold Continents (WACC)
412 pattern. On the other hand, Luo et al. (2019) established a causal chain from reduced sea ice to
413 reduced potential vorticity gradient and increased blocking events leading to cold extremes over
414 Eurasia. We computed the field average of blocking frequency within the domain of Peings
415 (2019) (10°W-80°E, 45-80°N) and could find a strong correlation with the WACC pattern over
416 time, however only for DJF blocking events (not shown). We find a correlation of November
417 UB events with wintertime NAO, which is however still weaker than the relationship with the
418 November snow dipole, as well as our BKS ice index (see Supplementary Figure 6). Moreover,
419 blockings within the domain of Peings (2019) (10°W-80°E, 45-80°N) are not related to a snow
420 dipole whatsoever, neither in October nor in November (see Supplementary Figure 6). That
421 said, we want to highlight the fact that the blocking pattern emerging in Figure 6 is mostly
422 outside of the boundaries of this UB index (10°W-80°E, 45-80°N), and thus might not be caught
423 by this recent study. Furthermore, Peings (2019) applies a very general snow cover increase in
424 his nudging experiment, rather than a snow dipole with a west to east gradient.

425 We also want to point out the possibility of ENSO contributing to a decadal November snow
426 signal. Strong La Niña events at the end of the 19th century as well as the strong El Niño events
427 between 1920–1940 seem to extend the periods of low and high snow beyond the frequency of
428 AMO. It is known that strong ENSO events that seem to have enough power to significantly
429 influence European climate (Domeisen et al. 2018) on an interannual basis. Moreover, recent
430 studies point towards possible links between the ENSO region, the Madden-Julian Oscillation
431 (MJO) and European climate (Kang and Tziperman 2017, Garfinkel et al. 2018). However,
432 more research is needed to make more confident statements about such teleconnections.



433 **Kolstad and Screen 2019** highlighted the importance of non-stationarity regarding Arctic sea
434 ice and mid-latitude climate variability. In our analysis, running correlations show interdecadal
435 variations concerning the strengths of November snow as the predictor for wintertime NAO.
436 Compared to the analysis of **Douville et al. (2017)**, we could strengthen the stationarity by
437 facilitating the November dipole snow, especially using 20CRv2c snow cover data, but the
438 question behind decadal peaks and valleys in the running correlation persist. To begin with, the
439 October and November snow indices show very different, nearly anticorrelated, running
440 correlation patterns. A high November snow index seems to be a strong predictor for a negative
441 NAO state at the beginning and end of the 20th century, as well as around the 1950s and 60s.
442 On the other hand, the October index, and related to that the results by **Douville et al. (2017)**,
443 shows negative correlations during the 1940s and 1980s.

444 We found the main reason for the reduction in correlation strength to be reduced variance of
445 the snow index time series during said time period (Figure 8). The reduction of variance is even
446 stronger in ERA20C than in 20CRv2c, which would explain the less stationary correlations in
447 ERA20C. Furthermore, such periods of low snow variability coincide with a reduction of polar
448 vortex variability, hinting even more so towards possible links between November snow and
449 stratospheric temperatures in the following month.

450 Overall, we advocate the importance of the signal-to-noise ratio rather than mean states for the
451 evolution of the November snow to winter NAO relationship. The general physical link seems
452 rather stable through time, but can be amplified (and dampened) by strong (weak) interannual
453 variability. What exactly causes the snow variability to drop is difficult to assess, but
454 preliminary results support the notion of low variability in AMO and sea ice concentration to
455 have an influence, which supports the above outlined mechanisms (not shown).

456 Another source of uncertainty is the disagreement between ERA20C and 20CRv2c when it
457 comes to the stationarity of the relationship. 20CRv2c shows negative correlation throughout
458 the whole 20th century, whereas ERA20C flips the sign of the correlation in the late 1930s and
459 late 1970s. The same relationship but using October snow shows high agreement between the
460 two datasets, which is the same case for the correlations between snow and stratospheric GPH.
461 We therefore conclude, that the information stored in the November snow cover in 20CRv2c is
462 slightly different to the information stored in the ERA20C snow depth. **Wegmann et al. (2017)**
463 found that Eurasian November snow depth shows much larger disagreement between 20CRv2c
464 and ERA20C than the same snow depth in October. Moreover, rather strong centennial trends
465 (although linear trend subtraction was done for this study) in ERA20C snow depth might impact

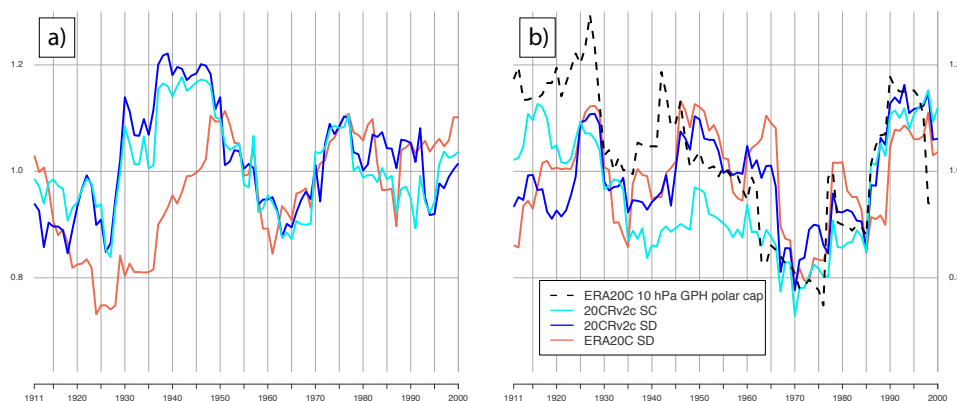


466 the running correlations. Finally, since snow depths are relatively low in October, differences
467 between using snow cover and snow depth might be less important from an energy transfer
468 point of view.

469 The disagreement between ERA20C and 20CRv2c may also be related to uncertainties and
470 inhomogeneities in both reanalyses. Many studies showed that both ERA20C and 20CRv2c are
471 not suitable for studies looking at trends (e.g. **Brönnimann et al., 2012; Krüger et al., 2013**)
472 and may include radical shifts in atmospheric circulation, particularly over the Arctic (e.g.
473 **Dell'Aquila et al., 2016; Rohrer et al., 2019**). **Rohrer et al. (2019)** showed that although
474 trends in centennial reanalyses may be spurious, at least in the Northern Hemisphere year-to-
475 year variability of mid-tropospheric circulation is in agreement even in the early 20th century.

476 Finally, although we focus here on the connection to the NAO, we did not find strong significant
477 correlations between autumn snow and winter WACC. As pointed out by **Peings (2019)**, the
478 most important driver for the WACC signal is the Ural blocking, for which we find strong
479 correlations throughout the 20th century (not shown).

480



481

482 *Figure 8: 21-year running standard deviation time series of a) October snow index and b) November snow index in ERA20C*
483 *and 20CRv2c (snow cover and snow depth). Dashed black line shows running standard deviation of 10 hPa November*
484 *December mean GPH over the polar regions.*

485

486

487 5. Conclusion

488 Several reconstruction and reanalysis datasets were used to examine the link between autumn
489 snow cover, ocean surface conditions and the NAO pattern in winter. We found evidence for a
490 manifestation of a negative NAO after November with a strong west-to-east snow cover



491 gradient, with this relationship being significant for the last 150 years. Nevertheless,
492 interdecadal variability for this relationship shows episodes of decreased correlation power,
493 which co-occur with episodes of low variability in the November snow index. This underlines
494 the importance of the signal-to-noise ratio for seasonal prediction studies.

495 Furthermore, our analysis of centennial time series supports studies pointing out the impact of
496 autumn snow on stratospheric circulation as well as the connection between reduced BKS ice
497 concentration and increased snow cover in eastern Eurasia. The latter mechanism is triggered
498 via the development of an atmospheric high-pressure anomaly adjacent to the BKS sea ice
499 anomaly, which transports moisture and cold air along its eastern flank into the continent. The
500 interdecadal evolution of the November snow index also points towards a co-dependence with
501 high North Atlantic SSTs subsequently reduced sea ice.

502 Extending the investigation period from 35 to 110 and up to 150 years increases the confidence
503 in recently proposed physical mechanisms behind cryospheric drivers of atmospheric
504 variability and decreases the probability of random co-variability between the Arctic
505 cryosphere changes and mid-latitude climate. Nevertheless, further model studies are needed to
506 investigate snow forcing for seasonal prediction to support the statistical links shown in this
507 study with causation. Future experiments should take into account year-to-year variability and
508 realistic distribution of snow cover if links to the stratosphere are to be examined.

509 For future studies regarding seasonal prediction, we emphasize the use of the November snow
510 dipole concerning a forecasting of the winter NAO state. Nevertheless, periods of weak
511 correlation might occur again, especially since it is uncertain how the sea ice to snow
512 relationship will change in the future, once the Arctic is ice free in summer or the local warming
513 is strong enough to override the counterintuitive snow cover increase. Thus, further studies are
514 needed to investigate the interplay between Arctic sea ice and continental snow distribution.

515 **Acknowledgements**

516 Marco Rohrer was supported by the Swiss National Science Foundation under Grant 143219.
517 The Twentieth Century Reanalysis Project datasets are supported by the U.S. Department of
518 Energy, Office of Science Innovative and Novel Computational Impact on Theory and
519 Experiment (DOE INCITE) program, and Office of Biological and Environmental Research
520 (BER), and by the National Oceanic and Atmospheric Administration Climate Program Office.
521 The ECMWF 20th Century Reanalyses and model simulations are supported by the EU FP7
522 project ERA-CLIM2.



523 **Data Availability**

524 The MERRA2 reanalysis data is publicly available at the NASA EARTHDATA repository
525 (<https://disc.gsfc.nasa.gov/daac-bin/FTPSubset2.pl>). The ERA-20C reanalysis data is publicly
526 available at the ECMWF data repository (<https://apps.ecmwf.int/datasets/>). The 20CRv2c
527 reanalysis data is publicly available at the NOAA Earth System Research Laboratory repository
528 (https://www.esrl.noaa.gov/psd/data/gridded/data.20thC_ReanV2c.html). The blocking
529 algorithm is publicly available at <https://github.com/marco-rohrer/TM2D>. The AMO
530 reconstruction data is a publicly available at the NOAA Earth System Research Laboratory
531 (<https://www.esrl.noaa.gov/psd/data/timeseries/AMO/>). The Niño 3.4 reconstruction is
532 publicly available at the GCOS Working Group on Surface Pressure repository
533 (https://www.esrl.noaa.gov/psd/gcos_wgsp/Timeseries/Nino34/). The NAO reconstruction is
534 publicly available at the Climate Research Unit repository
535 (<https://crudata.uea.ac.uk/cru/data/nao/>). The Walsh et al. sea ice concentration reconstruction
536 is publicly available at the National Snow and Ice Data Center repository
537 (<https://nsidc.org/data/g10010>).

538 **Author Contribution**

539 M.W. devised the study, the main conceptual ideas and the proof outline. M.R. assisted with
540 data availability and performed the blocking algorithm. M.W. wrote the manuscript in
541 consultation with M.S.-O. and G.L., who aided in interpreting the results.

542 **Competing interest**

543 The authors declare that they have no conflict of interest.

544 **References**

- 545 Allan, R., and T. Ansell, 2006: A New Globally Complete Monthly Gridded Mean
546 Sea Level Pressure Dataset (HadSLP2): 1850-2004. *J. Climate*, 19, 5816-5842.
- 547 Athanasiadis, P. J., Bellucci, A., Scaife, A. A., Hermanson, L., Materia, S., Sanna, A., ... and
548 Gualdi, S. (2017). A multisystem view of wintertime NAO seasonal predictions. *Journal*
549 *of Climate*, 30(4), 1461-1475.
- 550 Belleflamme A, Fettweis X, Erpicum M (2015) Recent summer Arctic atmospheric circulation
551 anomalies in a historical perspective. *Cryosphere* 9:53–64



- 552 Blackport, Russell, and James A. Screen. "Influence of Arctic Sea Ice Loss in Autumn
553 Compared to That in Winter on the Atmospheric Circulation." *Geophysical Research*
554 *Letters* 46.4 (2019): 2213-2221.
- 555 Blackport, R., Screen, J.A., van der Weil, K., and Bintanja, R. (2019). Minimal influence of
556 reduced Arctic sea ice on coincident cold winters in mid-latitudes. *Nature Climate*
557 *Change*, ?
- 558 Boland, E. J., Bracegirdle, T. J., and Shuckburgh, E. F. (2017). Assessment of sea ice-
559 atmosphere links in CMIP5 models. *Climate Dynamics*, 49(1-2), 683-702.
- 560 Brönnimann, S., Luterbacher, J., Staehelin, J., Svendby, T. M., Hansen, G., and Svenøe, T.
561 (2004). Extreme climate of the global troposphere and stratosphere in 1940–42 related to
562 El Niño. *Nature*, 431(7011), 971.
- 563 Brönnimann, S., Xoplaki, E., Casty, C., Pauling, A., and Luterbacher, J. (2007). ENSO
564 influence on Europe during the last centuries. *Climate Dynamics*, 28(2-3), 181-197.
- 565 Cohen, J., and Entekhabi, D. (1999). Eurasian snow cover variability and Northern Hemisphere
566 climate predictability. *Geophysical Research Letters*, 26(3), 345-348.
- 567 Cohen, J., Barlow, M., Kushner, P. J., and Saito, K. (2007). Stratosphere–troposphere coupling
568 and links with Eurasian land surface variability. *Journal of Climate*, 20(21), 5335-5343.
- 569 Cohen, J., Screen, J. A., Furtado, J. C., Barlow, M., Whittleston, D., Coumou, D., ... and Jones,
570 J. (2014). Recent Arctic amplification and extreme mid-latitude weather. *Nature*
571 *geoscience*, 7(9), 627.
- 572 Cohen, J. (2016). An observational analysis: Tropical relative to Arctic influence on midlatitude
573 weather in the era of Arctic amplification. *Geophysical Research Letters*, 43(10), 5287-
574 5294.
- 575 Cohen, J., Pfeiffer, K., and Francis, J. A. (2018). Warm Arctic episodes linked with increased
576 frequency of extreme winter weather in the United States. *Nature communications*, 9(1),
577 869.
- 578 Collow, T. W., Wang, W., Kumar, A., and Zhang, J. (2017). How well can the observed Arctic
579 sea ice summer retreat and winter advance be represented in the NCEP Climate Forecast
580 System version 2?. *Climate Dynamics*, 49(5-6), 1651-1663.



- 581 Cram, T. A., Compo, G. P., Yin, X., Allan, R. J., McColl, C., Vose, R. S., ... and Bessemoulin,
582 P. (2015). The international surface pressure databank version 2. *Geoscience Data*
583 *Journal*, 2(1), 31-46.
- 584 Crasemann, B., Handorf, D., Jaiser, R., Dethloff, K., Nakamura, T., Ukita, J., and Yamazaki,
585 K. (2017). Can preferred atmospheric circulation patterns over the North-Atlantic-
586 Eurasian region be associated with arctic sea ice loss?. *Polar Science*, 14, 9-20.
- 587 Dell'Aquila, A., Corti, S., Weisheimer, A., Hersbach, H., Peubey, C., Poli, P., ... and Simmons,
588 A. (2016). Benchmarking Northern Hemisphere midlatitude atmospheric synoptic
589 variability in centennial reanalysis and numerical simulations. *Geophysical Research*
590 *Letters*, 43(10), 5442-5449.
- 591 Deser, C., Hurrell, J. W., and Phillips, A. S. (2017). The role of the North Atlantic Oscillation
592 in European climate projections. *Climate dynamics*, 49(9-10), 3141-3157
- 593 Domeisen, D. I., Garfinkel, C. I., and Butler, A. H. (2019). The teleconnection of El Niño
594 Southern Oscillation to the stratosphere. *Reviews of Geophysics*.
- 595 Douville, H., Peings, Y., and Saint-Martin, D. (2017). Snow-(N) AO relationship revisited over
596 the whole twentieth century. *Geophysical Research Letters*, 44(1), 569-577.
- 597 Dunstone, N., Smith, D., Scaife, A., Hermanson, L., Eade, R., Robinson, N., ... and Knight, J.
598 (2016). Skilful predictions of the winter North Atlantic Oscillation one year
599 ahead. *Nature Geoscience*, 9(11), 809.
- 600 Enfield, D. B., Mestas-Núñez, A. M., and Trimble, P. J. (2001). The Atlantic multidecadal
601 oscillation and its relation to rainfall and river flows in the continental US. *Geophysical*
602 *Research Letters*, 28(10), 2077-2080.
- 603 Francis, J. A. (2017). Why are Arctic linkages to extreme weather still up in the air?. *Bulletin*
604 *of the American Meteorological Society*, 98(12), 2551-2557.
- 605 Furtado, J. C., Cohen, J. L., Butler, A. H., Riddle, E. E., and Kumar, A. (2015). Eurasian snow
606 cover variability and links to winter climate in the CMIP5 models. *Climate*
607 *dynamics*, 45(9-10), 2591-2605.
- 608 Furtado, J. C., Cohen, J. L., and Tziperman, E. (2016). The combined influences of autumnal
609 snow and sea ice on Northern Hemisphere winters. *Geophysical Research Letters*, 43(7),
610 3478-3485.



- 611 García-Serrano, J., Frankignoul, C., Gastineau, G., and De La Càmara, A. (2015). On the
612 predictability of the winter Euro-Atlantic climate: lagged influence of autumn Arctic sea
613 ice. *Journal of Climate*, 28(13), 5195-5216.
- 614 Garfinkel, C. I., Schwartz, C., Domeisen, D. I., Son, S. W., Butler, A. H., and White, I. P.
615 (2018). Extratropical Atmospheric Predictability From the Quasi-Biennial Oscillation in
616 Subseasonal Forecast Models. *Journal of Geophysical Research: Atmospheres*, 123(15),
617 7855-7866.
- 618 Gastineau, G., García-Serrano, J., and Frankignoul, C. (2017). The influence of autumnal
619 Eurasian snow cover on climate and its link with Arctic sea ice cover. *Journal of*
620 *Climate*, 30(19), 7599-7619.
- 621 Gelaro, R., McCarty, W., Suárez, M. J., Todling, R., Molod, A., Takacs, L., ... and Wargan, K.
622 (2017). The modern-era retrospective analysis for research and applications, version 2
623 (MERRA-2). *Journal of Climate*, 30(14), 5419-5454.
- 624 Ghatak, D., Frei, A., Gong, G., Stroeve, J., and Robinson, D. (2010). On the emergence of an
625 Arctic amplification signal in terrestrial Arctic snow extent. *Journal of Geophysical*
626 *Research: Atmospheres*, 115(D24).
- 627 Han, S., and Sun, J. (2018). Impacts of Autumnal Eurasian Snow Cover on Predominant Modes
628 of Boreal Winter Surface Air Temperature Over Eurasia. *Journal of Geophysical*
629 *Research: Atmospheres*, 123(18), 10-076.
- 630 Handorf, D., Jaiser, R., Dethloff, K., Rinke, A., and Cohen, J. (2015). Impacts of Arctic sea ice
631 and continental snow cover changes on atmospheric winter teleconnections. *Geophysical*
632 *Research Letters*, 42(7), 2367-2377.
- 633 Henderson, G. R., Peings, Y., Furtado, J. C., and Kushner, P. J. (2018). Snow-atmosphere
634 coupling in the Northern Hemisphere. *Nature Climate Change*, 1.
- 635 Honda, M., Inoue, J., and Yamane, S. (2009). Influence of low Arctic sea-ice minima on
636 anomalously cold Eurasian winters. *Geophysical Research Letters*, 36(8).
- 637 Hoshi, K., Ukita, J., Honda, M., Nakamura, T., Yamazaki, K., Miyoshi, Y., and Jaiser, R.
638 (2019). Weak Stratospheric Polar Vortex Events Modulated by the Arctic Sea-Ice
639 Loss. *Journal of Geophysical Research: Atmospheres*, 124(2), 858-869.
- 640 Hurrell, J. W., and Deser, C. (2010). North Atlantic climate variability: the role of the North
641 Atlantic Oscillation. *Journal of Marine Systems*, 79(3-4), 231-244.



- 642 Inoue, J., Hori, M. E., and Takaya, K. (2012). The role of Barents Sea ice in the wintertime
643 cyclone track and emergence of a warm-Arctic cold-Siberian anomaly. *Journal of*
644 *Climate*, 25(7), 2561-2568.
- 645 Jones, P. D., Jonsson, T., and Wheeler, D. (1997). Extension to the North Atlantic Oscillation
646 using early instrumental pressure observations from Gibraltar and south-west
647 Iceland. *International Journal of climatology*, 17(13), 1433-1450.
- 648 Jung, T., Vitart, F., Ferranti, L., and Morcrette, J. J. (2011). Origin and predictability of the
649 extreme negative NAO winter of 2009/10. *Geophysical Research Letters*, 38(7).
- 650 Kang, D., Lee, M. I., Im, J., Kim, D., Kim, H. M., Kang, H. S., ... and MacLachlan, C. (2014).
651 Prediction of the Arctic Oscillation in boreal winter by dynamical seasonal forecasting
652 systems. *Geophysical Research Letters*, 41(10), 3577-3585.
- 653 Kang, W., and Tziperman, E. (2017). More frequent sudden stratospheric warming events due
654 to enhanced MJO forcing expected in a warmer climate. *Journal of Climate*, 30(21),
655 8727-8743.
- 656 Kelleher, M., and Screen, J. (2018). Atmospheric precursors of and response to anomalous
657 Arctic sea ice in CMIP5 models. *Advances in Atmospheric Sciences*, 35(1), 27-37.
- 658 King, M. P., Hell, M., and Keenlyside, N. (2016). Investigation of the atmospheric mechanisms
659 related to the autumn sea ice and winter circulation link in the Northern
660 Hemisphere. *Climate dynamics*, 46(3-4), 1185-1195.
- 661 Kolstad, E. W., and Screen, J. A. (2019). Non-Stationary Relationship between Autumn Arctic
662 Sea Ice and the Winter North Atlantic Oscillation. *Geophysical Research Letters*.
- 663 Kretschmer, M., Coumou, D., Agel, L., Barlow, M., Tziperman, E., and Cohen, J. (2018).
664 More-persistent weak stratospheric polar vortex states linked to cold extremes. *Bulletin*
665 *of the American Meteorological Society*, 99(1), 49-60.
- 666 Laloyaux, P., de Boisseson, E., Balsaseda, M., Bidlot, J. R., Broennimann, S., Buizza, R., ...
667 and Kosaka, Y. (2018). CERA-20C: A coupled reanalysis of the Twentieth
668 Century. *Journal of Advances in Modeling Earth Systems*, 10(5), 1172-1195.
- 669 Luo, D., Chen, Y., Dai, A., Mu, M., Zhang, R., and Ian, S. (2017). Winter Eurasian cooling
670 linked with the Atlantic multidecadal oscillation. *Environmental Research*
671 *Letters*, 12(12), 125002.



- 672 Luo, D., Chen, X., Overland, J., Simmonds, I., Wu, Y., and Zhang, P. (2019). Weakened
673 potential vorticity barrier linked to recent winter Arctic sea-ice loss and mid-latitude cold
674 extremes. *Journal of Climate*, (2019).
- 675 McCusker, K. E., Fyfe, J. C., and Sigmond, M. (2016). Twenty-five winters of unexpected
676 Eurasian cooling unlikely due to Arctic sea-ice loss. *Nature Geoscience*, 9(11), 838.
- 677 Moore, G. W. K., and Renfrew, I. A. (2012). Cold European winters: interplay between the
678 NAO and the East Atlantic mode. *Atmospheric Science Letters*, 13(1), 1-8.
- 679 Mori, M., Kosaka, Y., Watanabe, M., Nakamura, H., and Kimoto, M. (2019). A reconciled
680 estimate of the influence of Arctic sea-ice loss on recent Eurasian cooling. *Nature*
681 *Climate Change*, 9(2), 123.
- 682 Orsolini, Y. J., and Kvamstø, N. G. (2009). Role of Eurasian snow cover in wintertime
683 circulation: Decadal simulations forced with satellite observations. *Journal of*
684 *Geophysical Research: Atmospheres*, 114(D19).
- 685 Orsolini, Y. J., Senan, R., Vitart, F., Balsamo, G., Weisheimer, A., and Doblas-Reyes, F. J.
686 (2016). Influence of the Eurasian snow on the negative North Atlantic Oscillation in
687 subseasonal forecasts of the cold winter 2009/2010. *Climate Dynamics*, 47(3-4), 1325-
688 1334.
- 689 Orsolini, Y., Wegmann, M., Dutra, E., Liu, B., Balsamo, G., Yang, K., ... and Senan, R. (2019).
690 Evaluation of snow depth and snow-cover over the Tibetan Plateau in global reanalyses using
691 in-situ and satellite remote sensing observations. *The Cryosphere*, 13, 2221–2239
- 692
- 693 Overland, J. E., Wood, K. R., and Wang, M. (2011). Warm Arctic—cold continents: climate
694 impacts of the newly open Arctic Sea. *Polar Research*, 30(1), 15787.
- 695 Overland, J. E., and Wang, M. (2018). Arctic-midlatitude weather linkages in North
696 America. *Polar Science*, 16, 1-9.
- 697 Pedersen, R. A., Cvijanovic, I., Langen, P. L., and Vinther, B. M. (2016). The impact of regional
698 Arctic sea ice loss on atmospheric circulation and the NAO. *Journal of Climate*, 29(2),
699 889-902.
- 700 Peings, Y., Brun, E., Mauvais, V., and Douville, H. (2013). How stationary is the relationship
701 between Siberian snow and Arctic Oscillation over the 20th century?. *Geophysical*
702 *Research Letters*, 40(1), 183-188.



- 703 Peings, Y., Douville, H., Colin, J., Martin, D. S., and Magnusdottir, G. (2017). Snow–(N) AO
704 teleconnection and its modulation by the Quasi-Biennial Oscillation. *Journal of*
705 *Climate*, 30(24), 10211-10235.
- 706 Peings, Y. (2019). Ural Blocking as a driver of early winter stratospheric
707 warmings. *Geophysical Research Letters*.
- 708 Petoukhov, V., and Semenov, V. A. (2010). A link between reduced Barents-Kara sea ice and
709 cold winter extremes over northern continents. *Journal of Geophysical Research:*
710 *Atmospheres*, 115(D21).
- 711 Poli, P., Hersbach, H., Dee, D. P., Berrisford, P., Simmons, A. J., Vitart, F., ... and Trémolet,
712 Y. (2016). ERA-20C: An atmospheric reanalysis of the twentieth century. *Journal of*
713 *Climate*, 29(11), 4083-4097.
- 714 Rayner, N. A. A., Parker, D. E., Horton, E. B., Folland, C. K., Alexander, L. V., Rowell, D. P.,
715 ... and Kaplan, A. (2003). Global analyses of sea surface temperature, sea ice, and night
716 marine air temperature since the late nineteenth century. *Journal of Geophysical*
717 *Research: Atmospheres*, 108(D14).
- 718 Rohrer, M., Brönnimann, S., Martius, O., Raible, C. C., Wild, M., and Compo, G. P. (2018).
719 Representation of extratropical cyclones, blocking anticyclones, and Alpine circulation
720 types in multiple reanalyses and model simulations. *Journal of Climate*, 31(8), 3009-
721 3031.
- 722 Rohrer, M., Broennimann, S., Martius, O., Raible, C. C., and Wild, M. (2019). Decadal
723 variations of blocking and storm tracks in centennial reanalyses. *Tellus A: Dynamic*
724 *Meteorology and Oceanography*, 71(1), 1-21.
- 725 Romanowsky, E., Handorf, D., Jaiser, R., Wohltmann, I., Dorn, W., Ukita, J., Cohen, J.,
726 Dethloff, K. and Rex, M. (2019). The role of stratospheric ozone for Arctic-midlatitude
727 linkages. *Scientific reports*, 9(1), 7962.
- 728 Ruggieri, P., Kucharski, F., Buizza, R., and Ambaum, M. H. P. (2017). The transient
729 atmospheric response to a reduction of sea-ice cover in the Barents and Kara
730 Seas. *Quarterly Journal of the Royal Meteorological Society*, 143(704), 1632-1640.
- 731 Saito, K., Cohen, J., and Entekhabi, D. (2001). Evolution of atmospheric response to early-
732 season Eurasian snow cover anomalies. *Monthly Weather Review*, 129(11), 2746-2760.



- 733 Scaife, A. A., Arribas, A., Blockley, E., Brookshaw, A., Clark, R. T., Dunstone, N., ... and
734 Hermanson, L. (2014). Skillful long-range prediction of European and North American
735 winters. *Geophysical Research Letters*, 41(7), 2514-2519.
- 736 Scaife, A. A., Karpechko, A. Y., Baldwin, M. P., Brookshaw, A., Butler, A. H., Eade, R., ...
737 and Smith, D. (2016). Seasonal winter forecasts and the stratosphere. *Atmospheric*
738 *Science Letters*, 17(1), 51-56.
- 739 Scherrer, S. C., Croci-Maspoli, M., Schwierz, C., and Appenzeller, C. (2006). Two-dimensional
740 indices of atmospheric blocking and their statistical relationship with winter climate
741 patterns in the Euro-Atlantic region. *International Journal of Climatology: A Journal of*
742 *the Royal Meteorological Society*, 26(2), 233-249.
- 743 Schwartz, C., and Garfinkel, C. I. (2017). Relative roles of the MJO and stratospheric variability
744 in North Atlantic and European winter climate. *Journal of Geophysical Research:*
745 *Atmospheres*, 122(8), 4184-4201.
- 746 Schwierz, C., Croci-Maspoli, M., and Davies, H. C. (2004). Perspicacious indicators of
747 atmospheric blocking. *Geophysical research letters*, 31(6).
- 748 Screen, J. A. (2017). Simulated atmospheric response to regional and pan-Arctic sea ice
749 loss. *Journal of Climate*, 30(11), 3945-3962.
- 750 Screen, J. A., Deser, C., Smith, D. M., Zhang, X., Blackport, R., Kushner, P. J., ... and Sun, L.
751 (2018). Consistency and discrepancy in the atmospheric response to Arctic sea-ice loss
752 across climate models. *Nature Geoscience*, 11(3), 155.
- 753 Smith, D. M., Scaife, A. A., Eade, R., and Knight, J. R. (2016). Seasonal to decadal prediction
754 of the winter North Atlantic Oscillation: emerging capability and future
755 prospects. *Quarterly Journal of the Royal Meteorological Society*, 142(695), 611-617.
- 756 Sorokina, S. A., Li, C., Wettstein, J. J., and Kvamstø, N. G. (2016). Observed atmospheric
757 coupling between Barents Sea ice and the warm-Arctic cold-Siberian anomaly
758 pattern. *Journal of Climate*, 29(2), 495-511.
- 759 Sun, C., Zhang, R., Li, W., Zhu, J., and Yang, S. (2019). Possible impact of North Atlantic
760 warming on the decadal change in the dominant modes of winter Eurasian snow water
761 equivalent during 1979–2015. *Climate Dynamics*, 1-11.



- 762 Suo, L., Gao, Y., Guo, D., Liu, J., Wang, H., and Johannessen, O. M. (2016). Atmospheric
763 response to the autumn sea-ice free Arctic and its detectability. *Climate Dynamics*, 46(7-
764 8), 2051-2066.
- 765 Thompson, D. W., and Wallace, J. M. (1998). The Arctic Oscillation signature in the wintertime
766 geopotential height and temperature fields. *Geophysical research letters*, 25(9), 1297-
767 1300.
- 768 Tibaldi, S., and Molteni, F. (1990). On the operational predictability of blocking. *Tellus*
769 *A*, 42(3), 343-365.
- 770 Trenary, L., and DelSole, T. (2016). Does the Atlantic Multidecadal Oscillation get its
771 predictability from the Atlantic Meridional Overturning circulation?. *Journal of*
772 *Climate*, 29(14), 5267-5280.
- 773 Tyrrell, N. L., Karpechko, A. Y., and Räisänen, P. (2018). The influence of Eurasian snow
774 extent on the northern extratropical stratosphere in a QBO resolving model. *Journal of*
775 *Geophysical Research: Atmospheres*, 123(1), 315-328.
- 776 Tyrrell, N. L., Karpechko, A. Y., Uotila, P., and Vihma, T. (2019). Atmospheric Circulation
777 Response to Anomalous Siberian Forcing in October 2016 and its Long-Range
778 Predictability. *Geophysical Research Letters*, 46(5), 2800-2810.
- 779 Vihma, T. (2014). Effects of Arctic sea ice decline on weather and climate: A review. *Surveys*
780 *in Geophysics*, 35(5), 1175-1214.
- 781 Walsh, J. E., Fetterer, F., Scott Stewart, J., and Chapman, W. L. (2017). A database for
782 depicting Arctic sea ice variations back to 1850. *Geographical Review*, 107(1), 89-107.
- 783 Wang, L., Ting, M., and Kushner, P. J. (2017). A robust empirical seasonal prediction of winter
784 NAO and surface climate. *Scientific reports*, 7(1), 279.
- 785 Wanner, H., Brönnimann, S., Casty, C., Gyalistras, D., Luterbacher, J., Schmutz, C., ... and
786 Xoplaki, E. (2001). North Atlantic Oscillation—concepts and studies. *Surveys in*
787 *geophysics*, 22(4), 321-381.
- 788 Warner, J. L. (2018). Arctic sea ice—a driver of the winter NAO?. *Weather*, 73(10), 307-310.
- 789 Wegmann, M., Orsolini, Y., Vázquez, M., Gimeno, L., Nieto, R., Bulygina, O., ... and Sterin,
790 A. (2015). Arctic moisture source for Eurasian snow cover variations in
791 autumn. *Environmental Research Letters*, 10(5), 054015.



- 792 Wegmann, M., Y. Orsolini, E. Dutra, O. Bulygina, A. Sterin, and S. Brönnimann, 2017:
793 Eurasian snow depth in long-term climate reanalyses. *Cryosphere*, 11, 923–935
- 794 Wegmann, M., Orsolini, Y., and Zolina, O. (2018a). Warm Arctic– cold Siberia: comparing the
795 recent and the early 20th-century Arctic warmings. *Environmental Research*
796 *Letters*, 13(2), 025009.
- 797 Wegmann, M., Dutra, E., Jacobi, H. W., and Zolina, O. (2018b). Spring snow albedo feedback
798 over northern Eurasia: Comparing in situ measurements with reanalysis
799 products. *Cryosphere*, 12(6).
- 800 Xu, B., Chen, H., Gao, C., Zhou, B., Sun, S., and Zhu, S. (2019). Regional response of winter
801 snow cover over the Northern Eurasia to late autumn Arctic sea ice and associated
802 mechanism. *Atmospheric Research*, 222, 100-113.
- 803 Yao, Y., Luo, D., Dai, A., and Simmonds, I. (2017). Increased quasi stationarity and persistence
804 of winter Ural blocking and Eurasian extreme cold events in response to Arctic warming.
805 Part I: Insights from observational analyses. *Journal of Climate*, 30(10), 3549-3568.
- 806 Yeo, S. R., Kim, W., and Kim, K. Y. (2017). Eurasian snow cover variability in relation to
807 warming trend and Arctic Oscillation. *Climate dynamics*, 48(1-2), 499-511.
- 808 Zhang, J., Tian, W., Chipperfield, M. P., Xie, F., and Huang, J. (2016). Persistent shift of the
809 Arctic polar vortex towards the Eurasian continent in recent decades. *Nature Climate*
810 *Change*, 6(12), 1094.
- 811